

Quantum dot spectroscopy using cavity QED

Martin Winger,¹ Antonio Badolato,¹ Kevin J. Hennessy,¹ Evelyn L. Hu,² and Ata Imamoğlu¹

¹*Institute of Quantum Electronics, ETH Zurich, 8093 Zurich, Switzerland*

²*California NanoSystems Institute, University of California, Santa Barbara, California 93106, USA*

(Dated: August 21, 2008)

Cavity quantum electrodynamics has attracted substantial interest, both due to its potential role in the field of quantum information processing and as a testbed for basic experiments in quantum mechanics. Here, we show how cavity quantum electrodynamics using a tunable photonic crystal nanocavity in the strong coupling regime can be used for single quantum dot spectroscopy. From the distinctive avoided crossings observed in the strongly coupled system we can identify the neutral and single positively charged exciton as well as the biexciton transitions. Moreover we are able to investigate the fine structure of those transitions and to identify a novel cavity mediated mixing of bright and dark exciton states, where the hyperfine interactions with lattice nuclei presumably play a key role. These results are enabled by a deterministic coupling scheme which allowed us to achieve unprecedented coupling strengths in excess of 150 μeV .

Cavity quantum electrodynamics (QED) studies the quantum limit of light-matter interaction in an optical cavity [1]; its implementation in both atomic [2] and solid state systems [3] has received substantial interest primarily due to potential applications in quantum information processing [1, 4]. Self-assembled quantum dots (QDs) embedded in monolithic nanocavities provide a well-controlled and robust system for conducting cavity QED experiments in the solid state. The combination of ultra-small mode volumes and high Q values provided by those systems has made it possible to enter the strong coupling regime of cavity QED with different types of monolithic cavities [5, 6, 7, 8]. However, in all previously reported experiments, a nanocavity mode was brought into resonance with a QD transition whose nature could not have been specified. This is mainly due to the fact that the inherently random excitation scheme used in photoluminescence (PL) spectroscopy allows for the creation of a multitude of QD charge configurations and the resulting spectral emission lines are generally difficult to interpret. This ambiguity has not hindered progress in the field since the emphasis has so far been on using the QD as a two-level emitter that couples resonantly to a nanocavity mode [9, 10]; the nature of the particular QD transition was irrelevant for the study of cavity-QED physics.

In contrast, we show here that a nanocavity mode that is strongly coupled to QD transitions can be used as a powerful spectroscopic tool for studying the fundamental properties of the QD itself. The distinct spectral anti-crossings observed when the cavity is tuned across resonance with different QD transitions allow us first of all to unambiguously identify the single (positively) charged exciton (X^+), the neutral exciton (X^0), and the neutral biexciton (XX^0) emission lines. Surprisingly, cavity-QED also allows us to study the fine structure of QD transitions and identify a novel strong coupling induced mixing of bright and dark exciton complexes.

In order to reach the strong coupling regime of cav-

ity QED the coherent coupling rate g between an excitonic transition and a cavity field has to exceed the decay rates of the exciton (Γ) and the cavity (κ), obeying $g > \Gamma/4, \kappa/4$ [11]. This is achieved in a deterministic fashion using the approach introduced in [8, 12] where cavities are precisely positioned around pre-selected QDs in order to achieve a maximum coupling strength. InAs QDs were grown by molecular beam epitaxy in the centre of a 126 nm thick GaAs membrane on top of a 1 μm thick $\text{Al}_{0.7}\text{Ga}_{0.3}\text{As}$ layer that allowed for subsequent cavity membrane formation. In situ annealing shifted the QD s-shell emission wavelength to $\lambda \simeq 940$ nm. We identified well-isolated QDs in PL and mapped them using atomic force microscopy. Around those QDs we then fabricated PC defect cavities in the L3 configuration [13] using electron beam lithography in combination with a dry and wet etching process. The effective mode volume of an L3 cavity is $V_{\text{eff}} = 0.7 \cdot (\lambda/n)^3$ and the theoretical Q-value is $Q = 3 \cdot 10^5$. In general, the positioning technique we use has a precision of approximately 30 nm. The device we study here has negligible misalignment between the QD and the field maximum of the first order cavity mode, such that we expect a maximum coherent coupling rate g .

In order to perform micro-PL studies at $T = 4.2$ K, the sample was mounted into a liquid Helium flow cryostat. For off-resonant excitation of the GaAs host material we used a titanium sapphire laser that could be either operated in continuous wave mode or mode-locked in order to emit picosecond pulses. The excitation laser beam was focused onto the PC cavity using a microscope objective with a numerical aperture of $NA = 0.55$. The luminescence signal was collected through the same microscope objective, coupled into a single mode fibre, and directed to a grating spectrometer for spectral analysis. A holographic grating with 1500 grooves per millimetre allowed for a spectral resolution of 30 μeV . The signal was detected with a liquid nitrogen cooled charge coupled device (CCD) camera. Moreover, a crystal polarizer in the de-

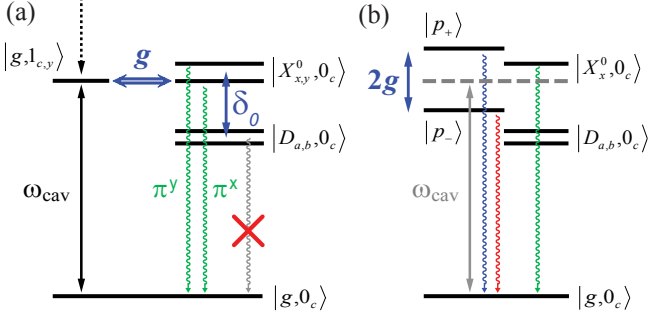


FIG. 1: X^0 level scheme. (a) Eigenstates of the QD and the one-photon state of the cavity mode. The electric field vector of the cavity field is parallel to the y-direction at the QD location, giving rise to coherent coupling g with $|X_y^0, 0_c\rangle$ while $|X_x^0, 0_c\rangle$ is not influenced by the cavity mode. (b) Dressed eigenstates of the coupled cavity-QD system. The polariton states $|p_+\rangle$ and $|p_-\rangle$ that are split by $2g$.

tection path allowed for doing polarization sensitive PL studies.

In the lowest energy conduction band states of a QD, electrons have spin z-component $S_{e,z} = \pm \frac{1}{2}$, while the (heavy) holes in the lowest energy valence-band states carry pseudospin $J_{h,z} = \pm \frac{3}{2}$. The light hole states with $J_{h,z} = \pm \frac{1}{2}$ are split off by > 35 meV and can therefore be neglected. The total angular momentum projection of the lowest energy electron-hole pairs (excitons) therefore can take the values $M = \pm 1, \pm 2$. The states with $M = \pm 2$ (dark excitons) can not recombine optically, since their decay requires an angular momentum transfer of $2\hbar$. The states with $M = \pm 1$ on the other hand, give rise to the X^0 luminescence. The electron-hole exchange interaction has the effect of (i) splitting dark and bright states by δ_0 on the order of $100 - 200$ μ eV and (ii) lifting the degeneracy of both bright and dark manifolds [14, 15, 16]. The coupled excitonic eigenstates then are $|D_{a,b}\rangle = (|+2\rangle \pm |-2\rangle)/\sqrt{2}$ for the dark exciton doublet and $|X_{x,y}^0\rangle = (|+1\rangle \pm |-1\rangle)/\sqrt{2}$ for the bright doublet. The latter decay by emitting photons that are linear polarized along either of the two QD axes (x, y). This level scheme is shown in figure 1(a) along with the lowest excited state $|g, 1_{c,y}\rangle$ of the cavity-mode containing a single photon.

The electric field of the cavity mode in the centre of the PC defect, i.e. at the location of the QD, is oriented along the y-direction (perpendicular to the L3 defect line). Therefore we assume maximum coupling g between the cavity single-photon state $|g, 1_{c,y}\rangle$ and $|X_y^0, 0_c\rangle$; the second bright exciton state $|X_x^0, 0_c\rangle$ is not coupled to the cavity. This is schematized in figure 1(b) where the dressed QD-cavity states are shown for the cavity on resonance with $|X_y^0, 0_c\rangle$. While the uncoupled state $|X_x^0, 0_c\rangle$ remains unchanged, $|X_y^0, 0_c\rangle$ hybridizes with $|g, 1_{c,y}\rangle$, thereby forming the polariton states $|p_{\pm}\rangle =$

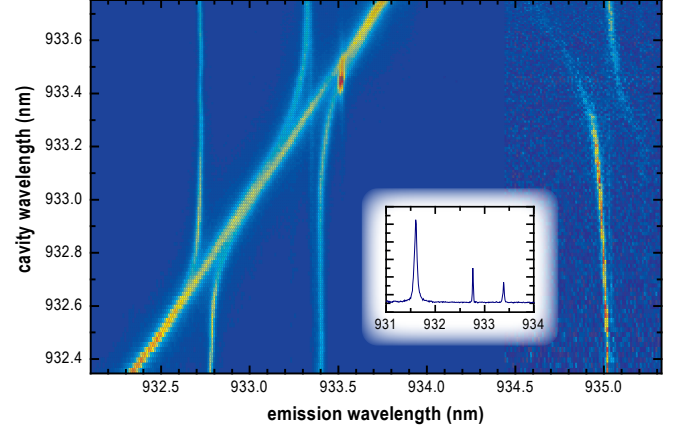


FIG. 2: Colour plot of PL spectra when tuning the cavity mode across the X^+ and the X^0 transitions. For both lines a clear anticrossing can be observed. The inset shows a typical PL spectrum for the cavity blue detuned from the X^+ line. The excitation conditions are $P_{ex} = 10$ nW and $\lambda_{ex} = 818$ nm. For wavelengths on the red of 934.5 nm the colour scale has been offset by a factor of 26 in order to highlight the biexciton emission.

$$(|X_y^0, 0_c\rangle \pm |g, 1_{c,y}\rangle)/\sqrt{2}.$$

The inset in figure 2(a) shows a typical PL spectrum obtained from a QD for a pump wavelength of $\lambda_{ex} = 818$ nm and a pump power of $P_{ex} = 10$ nW. We assign the line denoted with X^0 to spontaneous recombination of the states $|X_x^0, 0_c\rangle$ and $|X_y^0, 0_c\rangle$, which are typically split by $0 - 30$ μ eV. In the particular QD we study here, this splitting lies below the resolution of our spectral apparatus. The identification of this line as X^0 becomes obvious in the results presented below. Moreover we tentatively assign the line denoted by X^+ to emission from the positively charged exciton, where in addition to the electron-hole pair an extra hole is trapped within the QD. The splitting of 0.5 nm from the X^0 is in agreement with previous studies of similar QDs. We remark here that in order to obtain the PL spectrum depicted in the inset of figure 2(a), we had to carefully study the pump-wavelength dependence of the PL: we find that the strong cavity-feeding effect reported earlier [8] only allow the observation of strong QD transitions for a limited range of pump laser wavelengths.

The peak around 931.5 nm corresponds to emission from the uncoupled cavity mode. This feature can be perfectly fitted with a Lorentzian curve with a Q -factor of 16,000 which corresponds to a decay rate of $\kappa = 83$ μ eV. As has been shown in our previous work, efficient emission from the cavity mode is always present, irrespective of the detuning from QD spectral features [8]. Photon cross-correlation measurements revealed that this emission is solely due to the presence of a single QD in the PC membrane. The light emitted by the cavity is predominantly polarized along the y-direction (degree of polariza-

tion = 96%), i.e. perpendicular to the L3 defect direction.

In order to tune the cavity mode into resonance with the QD excitons, we employed a thin film gas-deposition technique to continuously red-shift the cavity mode wavelength [17, 18]. This technique allowed for a maximum tuning range of approximately 6 nm, sufficient to bring the cavity mode on resonance with both the X^+ and the X^0 lines of the QD. Figure 2 shows PL data for different cavity mode wavelengths in a colour plot. For each spectrum recorded, the central wavelength of the (uncoupled) cavity mode has been extracted and used to linearise the vertical axis. Furthermore, since the total intensity of the spectra fluctuates in time as a result of sample drift, each spectrum has been normalized to its integral. In the data shown here, the polarizer was oriented along the y-direction in order to maximize the signal from the cavity mode. As we cross the shorter wavelength line (X^+), we observe an anticrossing of the cavity and QD lines along with a central peak that corresponds to emission from the uncoupled cavity mode at times when the QD occupies a charging state other than the X^+ . The vacuum Rabi splitting on the X^+ line is found to be $2g = 205 \mu\text{eV}$. The strong coupling condition $g > \kappa/4, \Gamma/4$ is obviously well fulfilled for those parameter values. Moreover, we observe that the emission of the strongly coupled polariton doublet is co-polarized with the cavity mode.

As gas tuning proceeds, the cavity moves in resonance with the X^0 peak in the spectrum. The two anticrossing lines again correspond to emission from the polariton states $|p_{\pm}\rangle$ that here show a vacuum Rabi splitting of $2g = 316 \mu\text{eV}$, which is, to the best of our knowledge, the largest splitting reported so far in any cavity-QED system with a single emitter. The approximately 1.5 times larger coupling to this peak compared to the one observed with the X^+ line is consistent with our identification of this peak with the X^0 line and arises from the fact that the X^+ trion transitions are circularly polarized.

Furthermore, we observe that the neutral biexciton line XX^0 at $\lambda_{XX^0} = 935 \text{ nm}$ undergoes a splitting as the cavity is on resonance with the X^0 . This can clearly be seen as the anticrossing feature around that wavelength in figure 2. Since the pump power here is well below the saturation of the QD, emission from the XX^0 is rather weak. For this reason the colour scale of figure 2 has been offset for wavelengths longer than 934.5 nm. Since the XX^0 emission occurs via decay of the biexciton state to the neutral exciton $|X_{x,y}^0\rangle$ states, the vacuum Rabi splitting of the $|X_y^0\rangle$ state leads to a splitting in the XX^0 line. The upper (lower) polariton state shifts the biexciton decay to lower (higher) emission energy: therefore, the anticrossing feature of XX^0 appears horizontally flipped with respect to that of the X^0 . Since the PL data shown here is obtained using a polarizer that was oriented along the y-direction, the unsplit XX^0 emission to the $|X_x^0\rangle$ state is not observable.

The splitting of the two anticrossing XX^0 branches

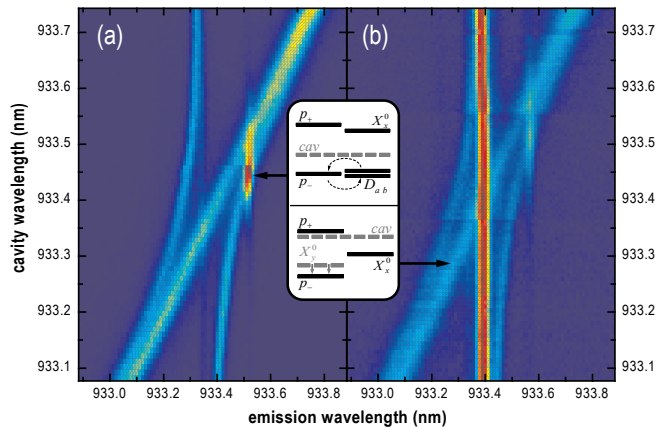


FIG. 3: Comparison of X^0 dynamics for different emission polarization (a) Zoomed-in version of figure 2 for the polarizer set in order to maximize cavity emission. The inset shows level schemes for two different positions of the cavity mode. In the lower inset the cavity is red-detuned from the X^0 . As the cavity photon energy is reduced, $|p_{-}\rangle$ moves in resonance with the dark states $|D_{a,b}\rangle$ as indicated in the upper inset. (b) Here the polarizer is set to 55° with respect to the cavity emission. Here the PL is plotted in a logarithmic colour scale.

amounts to 0.22 nm, identical to the vacuum Rabi splitting of the X^0 itself. Moreover, the intensity of the cavity-like branches decays when moving away from resonance. This is exactly the behaviour expected from the XX^0 decaying to the QD-like component of the intermediate polariton states $|p_{\pm}\rangle$. Furthermore, we note that there is no signature of an uncoupled cavity peak as in the anticrossing features observed on the X^+ and X^0 lines. This supports the hypothesis that its appearance in the latter is not an intrinsic feature of the resonantly coupled QD-cavity system itself, but rather a manifestation of off-resonant cavity feeding at times when the QD occupies a charging state other than the one the cavity is resonantly coupled to.

In comparison to the anticrossing observed on the X^+ line, the resonant signature on X^0 shows additional features. First we notice that there is a weak additional emission line that does not shift as the cavity is tuned across resonance. This emission can be attributed to the uncoupled state $|X_x^0, 0_c\rangle$, the dipole of which is orthogonal to the cavity electric field such that it does not interact with the cavity mode. Further evidence comes from the polarization behaviour of the emission: As the polarizer in the detection path is rotated, the emission from this central line increases and dominates the spectrum for a polarization setting orthogonal to the cavity mode emission. Figure 3 shows a zoom-in of the X^0 strong coupling feature for two different polarizations. In figure 3(a) the polarizer is oriented parallel to the cavity mode emission direction, whereas in 3(b) it is rotated by 55° , in order to make emission from both the uncoupled

exciton and the polariton features visible in the same spectrum.

A corresponding fine structure can be observed on the biexciton line, in that the anticrossing induced by vacuum Rabi splitting of the X^0 is only observed for a polarization parallel to the cavity mode (not shown in Fig. 3). The other pathway for biexciton decay leads through the intermediate state $|X_x^0\rangle$ which does not couple to the cavity. Therefore we also observe an x-polarized uncoupled biexciton line that does not shift as the cavity mode is being tuned. The presence of an uncoupled exciton and biexciton lines for x-polarized PL along with the correlated anticrossings of the y-polarized X^0 and the XX^0 emission lines make the identification of the neutral and biexciton transitions unambiguous.

We note that the behaviour of the X^0 line differs significantly from that of the X^+ line. In particular, for the X^+ transition there is no uncoupled exciton, as is expected for a charged exciton state. Due to the zero total spin-projection of the holes in the initial state of the X^+ decay, no exchange splitting occurs for the positively charged exciton. The two possible electron spin configurations then lead to degenerate circularly polarized transitions, either of which couple with equal strength to the cavity field. As decay then proceeds mainly via the cavity mode, the emission is co-polarized with the cavity mode for both initial spin configurations. Experimentally, we confirmed that there is no unsplit X^+ line by observing identical anticrossing features in both polarization channels.

As tuning proceeds further to the red side of the X^0 line, an unexpected feature appears in the PL. At $\lambda_0 = 933.52$ nm an additional line becomes activated as it is tuned into resonance with the lower polariton branch $|p_-\rangle$. We can rule out the possibility that this line arises from an unidentified charge configuration of the QD, since this additional PL peak shows a pronounced maximum for a resonance condition with the lower polariton state rather than with the uncoupled cavity mode. This suggests that the mechanism responsible for inducing this luminescence stems from the excitonic component of the polariton state $|p_-\rangle$.

We argue that this PL peak is due to neutral dark exciton states, activated by a combination of strong-coupling induced resonance between the bright-polariton and dark-exciton states, and an efficient elastic spin-flip scattering process. As the lower polariton state $|p_-\rangle$ is red shifted due to level repulsion, it approaches the doublet of dark excitons $|D_{a,b}\rangle$; the large cavity-exciton coupling ensures that the $|p_-\rangle$ state has substantial excitonic component when it reaches exact resonance with the dark-exciton transition. A sketch of this situation is given in the insets of figure 3: here resonance between the lower polariton and the dark excitons is achieved for a cavity position of $\lambda_{\text{cav}} = 933.45$ nm. The energy splitting between bright and dark exciton lines is found to

be $\delta_0 = 256\mu\text{eV}$, in good agreement with values of δ_0 reported elsewhere [19]. Furthermore, we have independently determined δ_0 from the splitting of the double negative charged exciton X^{2-} and the single negative charged biexciton $2X^{-1}$ as proposed in [20]. We identify those lines from their spectral locations and their power dependencies and determine an expected splitting of 0.17 nm, in close agreement to the measurements presented in figures 2 and 3.

In the off-resonant excitation scheme employed in our PL measurement, bright and dark excitons are populated with comparable probabilities, as carriers of random spin are injected into the QD. Optical decay of the population stored in the dark excitons however requires a spin-flip to take place prior to the optical recombination event. The strong dependence of the dark exciton PL on the detuning from the lower polariton branch observed here suggests that an elastic spin-flip process is involved in the optical activation of dark exciton decay. A strong candidate for this mechanism is the hyperfine interaction between the electron in the QD and the spins of the lattice nuclei. In this process the electron in the QD can exchange angular momentum with the lattice nuclei with negligible energy transfer [21]. This process is very inefficient for a QD outside a cavity, as the exchange energy δ_0 has to be overcome in order to flip the electron spin. However, as δ_0 is compensated by the strong-coupling induced shift of $|p_-\rangle$, we expect a significant increase of the hyperfine induced electron spin flip rate.

Typical hyperfine interaction strengths are on the order of $\Omega_N \simeq 0.5\mu\text{eV}$ for QDs with $\simeq 10^5$ atoms [21]. The effective optical recombination time of dark excitons via the resonant intermediate lower polariton state $|p_-\rangle$ then is given by $\gamma_p/\Omega_N^2 \simeq 110$ ns, where γ_p is the linewidth of the lower polariton. This timescale is relatively long compared to the < 100 ps timescale of polariton recombination and the $\simeq 10$ ns timescale of the uncoupled exciton within the photonic bandgap. However, both bright and dark excitons are created with equal probability in the QD, such that the populations of the two are comparable for pump powers well below saturation. Even for different decay times this then leads to comparable PL intensities of the cavity induced dark exciton luminescence and the PL from the polariton states, which we confirm by multi-Lorentzian fits to our data. We note that as the pump power is increased, the dark excitons can make transitions to other charge configurations by the capture of additional carriers, which results in a depletion of the dark exciton population. In this case we expect a reduced strength of the cavity mediated dark exciton PL. Indeed we have verified this from power dependent measurements on a control device.

In conclusion we show that the strong-coupling limit of cavity QED can be used as a powerful spectroscopic tool, providing an unambiguous identification of QD spectral features. Our findings could prove to be useful in more

complicated systems such as coupled-QDs where the multitude of emission lines render precise identification of PL lines more difficult.

The authors would like to acknowledge Andreas Reinhard for many helpful discussions. This work is supported by NCCR Quantum Photonics (NCCR QP), research instrument of the Swiss National Science Foundation (SNSF).

-
- [1] Mabuchi, H. & Doherty, A. C. Cavity quantum electrodynamics: Coherence in context. *Science* **298**, 1372-1377 (2002).
 - [2] Raimond, J. M., Brune, M. & Haroche, S. Manipulating quantum entanglement with atoms and photons in a cavity. *Rev. Mod. Phys.* **73**, 565-582 (2001).
 - [3] Michler, P. *et al.* A quantum dot single-photon turnstile device. *Science* **290**, 2282-2285 (2000).
 - [4] Imamoglu, A. *et al.* Quantum information processing using quantum dot spins and cavity QED. *Phys. Rev. Lett.* **83**, 4204-4207 (1999).
 - [5] Yoshie, T. *et al.* Vacuum Rabi splitting with a single quantum dot in a photonic crystal nanocavity. *Nature* **432**, 200-203 (2004).
 - [6] Peter, E. *et al.* Exciton-photon strong-coupling regime for a single quantum dot embedded in a microcavity. *Phys. Rev. Lett.* **95**, 067401 (2005).
 - [7] Reithmaier, J. P. *et al.* Strong coupling in a single quantum dot-semiconductor microcavity system. *Nature* **432**, 197-200 (2004).
 - [8] Hennessy, K. *et al.* Quantum nature of a strongly coupled single quantum dot-cavity system. *Nature* **445**, 896-899 (2007).
 - [9] Englund, D. *et al.* Controlling cavity reflectivity with a single quantum dot. *Nature* **450**, 857-861 (2007).
 - [10] Srinivasan, K. & Painter, O. Linear and nonlinear optical spectroscopy of a strongly coupled microdisk-quantum dot system. *Nature* **450**, 862-866 (2007).
 - [11] Andreani, L. C., Panzarini, G. & Gérard, J.-M. Strong-coupling regime for quantum boxes in pillar microcavities: theory. *Phys. Rev. B* **60**, 13276-13279 (1999).
 - [12] Badolato, A. *et al.* Deterministic coupling of single quantum dots to single nanocavity modes. *Science* **308**, 1158-1161 (2005).
 - [13] Akahane, Y., Asano, T., Song, B. S. & Noda, S. High-Q photonic nanocavity in a two-dimensional photonic crystal. *Nature* **425**, 944-947 (2003).
 - [14] Bayer, M. *et al.* Fine structure of neutral and charged excitons in self-assembled In(Ga)As/(Al)GaAs quantum dots. *Phys. Rev. B* **65**, 195315 (2002).
 - [15] Ivchenko, E. L. Fine structure of excitonic levels in semiconductor nanostructures. *Phys. Stat. Sol. A* **164**, 487-492 (1997).
 - [16] Bester, G., Nair, S. & Zunger, A. Pseudopotential calculation of the excitonic fine structure of million-atom self-assembled In_{1-x}Ga_xAs/GaAs quantum dots. *Phys. Rev. B* **67**, 161306 (2003).
 - [17] Strauf, S. *et al.* Frequency control of photonic crystal membrane resonators by monolayer deposition. *Appl. Phys. Lett.* **88**, 043116 (2006).
 - [18] Srinivasan, K. & Painter, O. Optical fiber taper coupling and high-resolution wavelength tuning of microdisk resonators at cryogenic temperatures. *Appl. Phys. Lett.* **90**, 031114 (2007).
 - [19] Stevenson, R. M. *et al.* Magnetic-field-induced reduction of the exciton polarization splitting in InAs quantum dots. *Phys. Rev. B* **73**, 033306 (2006).
 - [20] Urbaszek, B. *et al.* Fine structure of highly charged excitons in semiconductor quantum dots. *Phys. Rev. Lett.* **90**, 247403 (2003).
 - [21] Merkulov, I. A., Efros, Al. L. & Rosen, M. Electron spin relaxation by nuclei in semiconductor quantum dots. *Phys. Rev. B* **65**, 205309 (2002).